JOURNAL OF NATURAL PRODUCTS

pubs.acs.org/jnp

Article

Neuroprotective Effects of Triterpenoids from *Camellia japonica* against Amyloid β-Induced Neuronal Damage

Hyo-Moon Cho, Thi-Kim-Quy Ha, Thi-Phuong Doan, Basanta Dhodary, Jin-Pyo An, Ba-Wool Lee, Jun-Li Yang, and Won-Keun Oh*

Cite This: *J. Nat. Prod.* 2020, 83, 2076−2086

Read Online

ACCESS | Metrics & More | Article Recommendations | Supporting Information

ABSTRACT: Alzheimer's disease (AD), a neurocognitive impairment affecting human mental capacity, is related to the accumulation of amyloid-β peptide (Aβ) and the hyperphosphorylation of tau protein. In addition to modern therapies approved for AD treatment, natural products with antioxidant and anti-inflammatory properties have been studied for their potential to prevent AD pathogenesis. Six new noroleanane triterpenoids from the fruit peels of *Camellia japonica* were isolated, and their structures were determined by diverse spectroscopic methods. The neuroprotective effects of the six new compounds were tested against Aβ-induced neurotoxicity and neuroinflammation in mouse hippocampal and microglial cells. In the model of HT22-transfected cells, compounds **1**−**4** showed strongly neuroprotective effects via antioxidant response element gene activation and decreased the level of glutamate uptake. Compounds **1**−**4** also appeared to have strong inhibitory effects on NO production in Aβ_{1-42}-transfected BV2 microglial cells. A docking simulation study was used to explain the inhibitory effects of compounds **1**−**4** on β-secretase 1 (BACE1). Noroleanane triterpenoids **1**−**4** had potential neuroprotective and anti-inflammatory effects against Aβ-induced neuronal damage. The structure−activity relationships of the 30 oleanane triterpenoids from *C. japonica* were assessed in a model of Aβ_{1-42}-transfected HT22 cells.

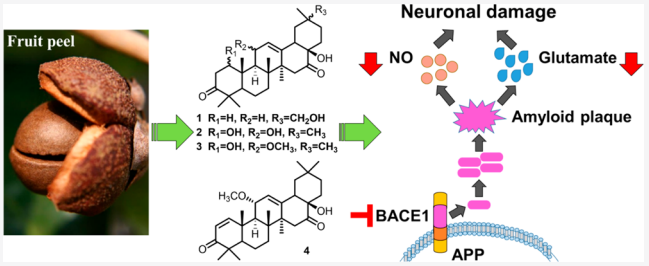

Alzheimer's disease is a neurological cognitive disorder caused by chronic neurodegeneration. The characteristic neuropathology of this disease involves the accumulation of amyloid-β peptide (Aβ), which forms extracellular plaques and intracellular tangles, and the hyperphosphorylation of tau protein.[1] The cause of Aβ-induced toxicity and neuroinflammation in AD pathogenesis has been suggested.[2] The aggregation of Aβ in the brain could disrupt intracellular Ca^{2+} homeostasis and promote free radical generation via the release of various inflammatory cytokines.[3−6] This series of events ultimately results in oxidative stress, which leads to inflammation and apoptosis of brain cells.[3,4] Therefore, strategies for protecting against Aβ-induced neurotoxicity and neuroinflammation may be therapeutic targets for the prevention and treatment of AD.

Aβ-induced neurotoxicity in immortalized mouse hippocampal HT22 cells has been developed as an in vitro model of neurodegenerative processes.[7] Microglial BV2 cells, a type of principal central nervous system (CNS) immune cells, also play an essential role in brain inflammation.[8] The accumulation of Aβ peptides in the AD brain is an important trigger for microglial activation. When AD is persistent and worsening, microglial cells are chronically activated, resulting in the production of a variety of pro-inflammatory cytokines and neurotoxic compounds, including interleukin-1β (IL-1β), IL-6, tumor necrosis factor-alpha (TNF-α), nitric oxide (NO), and reactive oxygen species (ROS). Therefore, these inflammatory mediators have injurious effects on neurodegenerative diseases and may result in brain damage.[9,10]

Natural products are a source of potential pharmacological agents with an abundance of novel chemical entities with various biological activities. In addition to the modern therapies approved for treatment of AD, natural products with antioxidant and anti-inflammatory properties have been studied as potential therapeutic agents against AD pathogenesis.[11,12] *Camellia japonica* L., an evergreen tree of the family Theaceae that is widely distributed in Korea, Japan, and China, has long been used as an anti-inflammatory, somatic agent, tonic, and treatment for the vomiting of blood and bleeding.[13] Potential inhibitory effects on porcine epidemic diarrhea virus (PEDV) and protein tyrosine phosphatase 1B (PTB1B) of oleanane triterpenoids isolated from the flowers and fruit peels of *C. japonica* were found.[14,15] In addition, *seco*-noroleanane triterpenoids from flowers showed protection

Received: October 5, 2019
Published: June 22, 2020

https://dx.doi.org/10.1021/acs.jnatprod.9b00964
J. Nat. Prod. 2020, 83, 2076−2086

against neurotoxicity in a rotenone model of Parkinson's disease.[12] Based on these previous studies, the history of folk medicine, and biological screening of *C. japonica* extract, the neuroprotective effects against Alzheimer's disease were investigated. This study demonstrated the neuroprotective effects of six new triterpenoids (**1**−**6**) from the fruit peels of *C. japonica* against Aβ- and glutamate-induced cytotoxicity. Furthermore, 24 known compounds isolated from *C. japonica* provided by the Korea Bank of Natural Materials (KBNMB) and six new compounds (**1**−**6**) were evaluated in a model of Aβ_{1-42}-transfected HT22 cells, and the structure−activity relationships (SARs) are discussed.

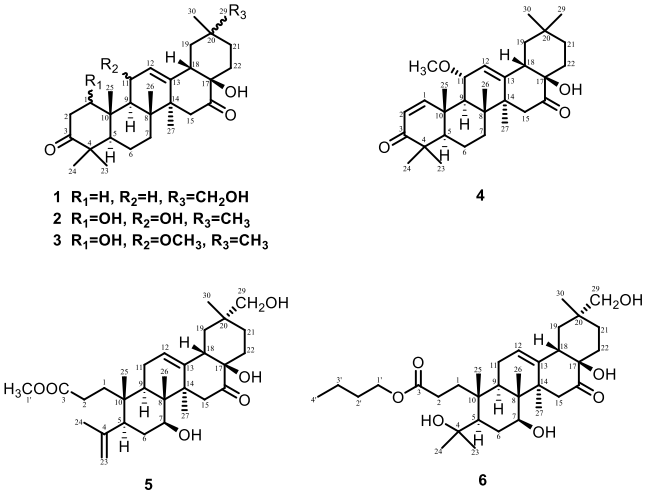

RESULTS AND DISCUSSION

A 70% EtOH extract of the fruit peels of *C. japonica* was separated by various chromatographic methods, including on silica gel, RP-C_{18}, Sephadex LH-20, and prep-HPLC columns, to afford four new 28-noroleanane-type (**1**−**4**) and two new 3,4-*seco*-28-noroleanane-type triterpenoids (**5** and **6**) (Figure 1).

Compound **1** was obtained as a white amorphous powder with $[\alpha]_D^{25}$ −29 (*c* 0.1, MeOH). The molecular formula of $C_{29}H_{44}O_4$ was determined from its positive ion HRESIMS data at *m*/*z* 439.3209 $[M + H - H_2O]^+$ (calcd for $C_{29}H_{43}O_3$, 439.3207). Its IR spectrum showed the presence of hydroxy (3414 cm^{-1}), carbonyl (1702 cm^{-1}), and olefinic (1457 cm^{-1}) functionalities. The ^1H NMR spectrum showed signals for six methyl groups at δ_H 1.17 (6H), 1.11, 1.06, 1.03, and 0.96, a hydroxymethyl (δ_H 3.16, 2H, t, *J* = 5.6 Hz, H_2-29), and an olefinic proton (δ_H 5.43, 1H, t, *J* = 3.6 Hz, H-12) (Table 1). The ^{13}C NMR spectrum revealed the presence of two carbonyl carbons at δ_C 216.0 (C-3) and 213.9 (C-16), two olefinic carbons at δ_C 143.0 (C-13) and 124.4 (C-12), a hydroxymethyl (δ_C 73.9, C-29), and an oxygenated tertiary carbon at δ_C 77.2 (C-17) (Table 2). This compound was proposed to possess an oleanane triterpenoid skeleton with six methyl groups and a 29-hydroxymethyl group based on the HSQC and HMBC spectra. The positions of the carbonyls at C-3 and C-16 and the oxygenated tertiary carbon at C-17 were confirmed by the HMBC correlations from H_2-1 (δ_H 1.90, 1.49), H_2-2 (δ_H 2.54, 2.33), Me-23 (δ_H 1.03), and Me-24 (δ_H 1.06) to C-3; from H_2-15 (δ_H 3.32, 1.62) and H-18 (δ_H 2.81) to C-16; and from H_2-15 and H-18 to C-17, respectively. These results suggested that **1** resembled those of the 29-hydroxymethyl derivative of camelledionol.[14] The 29-hydroxymethyl group was also confirmed by the HMBC cross-peaks from H_2-29 to C-20 and C-21 (δ_C 36.6 and 32.2, respectively) (Figure 1A). The coupling between H-9 and H-11β (*J* = 11.6 Hz) suggested a *trans*-diaxial configuration, and the α-orientations of H-5, H-9, and Me-27 were supported by the NOESY correlations from H-9 (δ_H 1.70) to H-5 (δ_H 1.44) and Me-27 (δ_H 1.17) (Figure 1B). Similarly, the coupling constants of H-18 (dd, *J* = 14.2, 4.2 Hz) and NOESY correlations from H-18 to Me-30 (δ_H 0.96) and HO-17 (δ_H 4.29) suggested a β-orientation for H-18. Thus, the structure of compound **1** was determined as 17β,29-dihydroxy-3,16-dioxo-28-norolean-12-ene.

Compound **2**, a white amorphous powder with $[\alpha]_D^{25}$ −15 (*c* 0.1, MeOH), had a molecular formula of $C_{29}H_{44}O_5$ based on its positive HRESIMS ion at *m*/*z* 473.3274 $[M + H]^+$ (calcd for $C_{29}H_{45}O_5$, 473.3267). The IR absorption bands showed the presence of hydroxy (3392 cm^{-1}), carbonyl (1713 cm^{-1}), and olefinic (1461 cm^{-1}) functionalities. Its ^1H and ^{13}C NMR data (Tables 1 and 2) showed that compound **2** was structurally similar to **1**. The differences between **1** and **2** were the presence of hydroxy groups at C-1 (δ_H 3.88, 1H, t, *J* = 6.9 Hz; δ_C 79.1) and C-11 (δ_H 4.34, 1H, dd, *J* = 8.5, 3.7 Hz; δ_C 67.3) as well as a Me-29 (δ_H 0.89, 3H, s; δ_C 32.9) instead of a hydroxymethyl group in **1**. These features were confirmed based on HSQC and HMBC experiments (Figure 1 and Figures S10 and S11, Supporting Information). The HMBC correlations from H-11 to C-12 (δ_C 127.5) and C-9 (δ_C 55.6) and from H-1 to C-2 (δ_C 43.8), C-3 (δ_C 217.5), and C-25 (δ_C 12.4) suggested that the hydroxy groups were at C-1 and C-11. HMBC cross-peaks from Me-29 to C-20 (δ_C 31.6) and C-21 (δ_C 37.7) were consistent with the presence of the methyl group at C-29. The relative configuration of **2** was determined by comparing NOESY data (Figure 1B) and coupling constants with compound **1**. The β-orientation of HO-1 was identified based on the correlations from H-9 (δ_H 1.77) to H-1 and Me-27 (δ_H 1.26). Thus, the structure of compound **2** was defined as 1β,11α,17β-trihydroxy-3,16-dioxo-28-norolean-12-ene.

Compound **3**, a white amorphous powder with $[\alpha]_D^{25}$ −40 (*c* 0.1, MeOH), was determined to have the molecular formula $C_{30}H_{46}O_5$ based on its positive HRESIMS ion at *m*/*z* 509.3198 $[M + Na]^+$ (calcd for $C_{30}H_{46}NaO_5$, 509.3237). Its IR absorption bands showed the presence of hydroxy (3566 cm^{-1}), carbonyl (1744 cm^{-1}), and olefinic (1595 cm^{-1}) functionalities. The ^1H and ^{13}C NMR data (Tables 1 and 2) were highly similar to those of **2** except that HO-11 in **2** was replaced by MeO-11 (δ_H 3.34, 3H, s) in **3**. The position of the methoxy group at C-11 was confirmed by the HMBC cross-peak from the methoxy hydrogens to C-11 (δ_C 75.8). (Figure 1A). The NOESY correlations from H-11 (δ_H 4.39) to Me-25 (δ_H 1.20) and Me-26 (δ_H 1.07) confirmed the 11α-methoxy group. Accordingly, the structure of compound **3** was defined as 1β,17β-dihydroxy-11α-methoxy-3,16-dioxo-28-norolean-12-ene.

Compound **4** was obtained as a white amorphous powder with $[\alpha]_D^{25}$ +21 (*c* 0.1, MeOH). Its negative ion HRESIMS data indicated the presence of an $[M + HCOO]^-$ ion at *m*/*z* 513.3223 (calcd for $C_{31}H_{45}O_6$, 513.3222), corresponding to the molecular formula $C_{30}H_{44}O_4$. Its IR spectrum showed the presence of hydroxy (3586 cm^{-1}), carbonyl (1748 cm^{-1}), and olefinic (1596 cm^{-1}) functionalities. The ^1H and ^{13}C NMR data (Tables 1 and 2) were similar to those of compound **3**,

https://dx.doi.org/10.1021/acs.jnatprod.9b00964
J. Nat. Prod. 2020, 83, 2076−2086

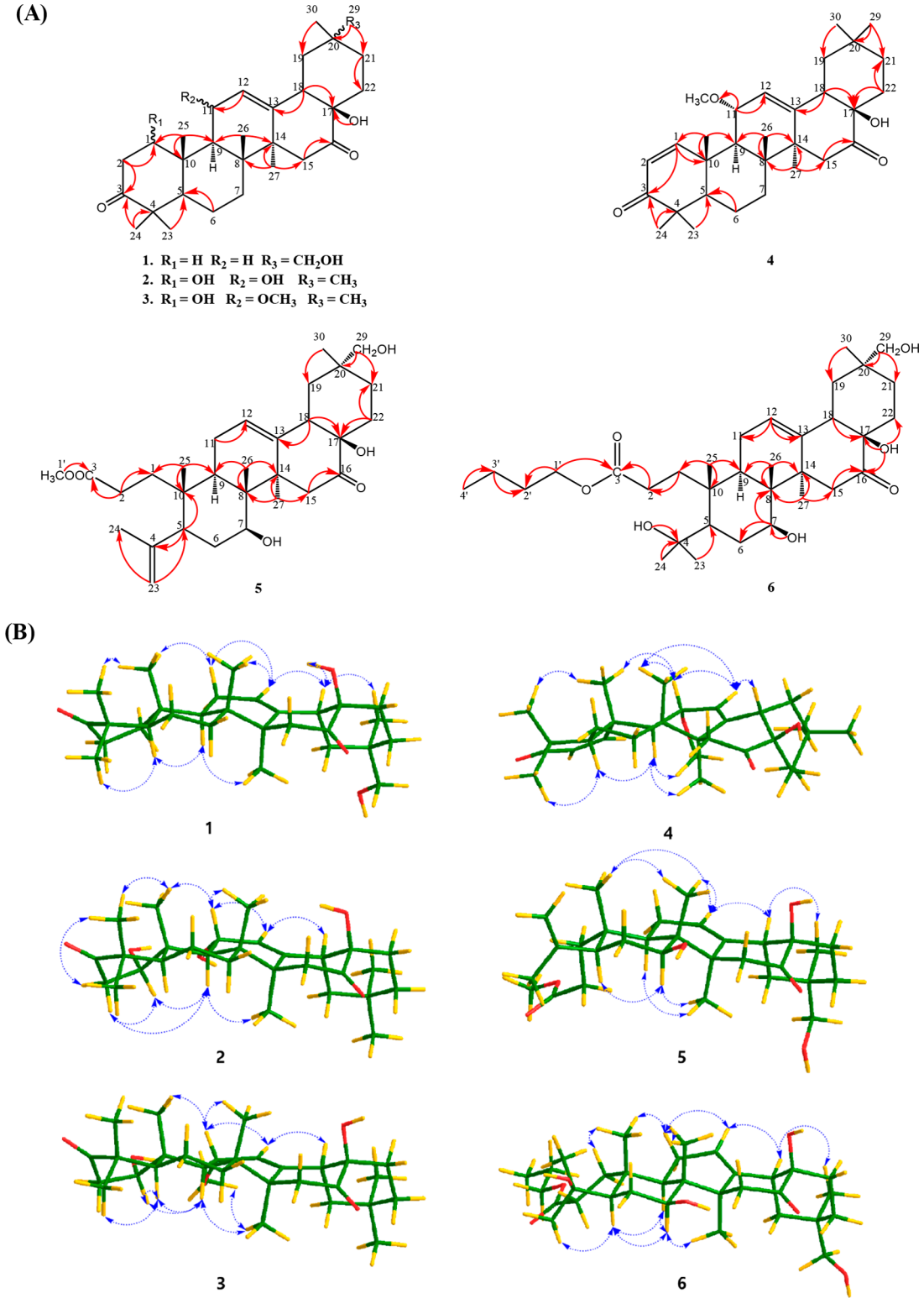

Figure 1. (A) Key HMBC (red arrows) correlations of compounds **1**−**6**. (B) Key NOESY correlations (dashed arrows) of compounds **1**−**6**.

and the spectra showed two carbonyl carbons (δ_C 215.6 and 207.3), a trisubstituted double bond [δ_H 5.67, 1H, d, J = 3.4 Hz; δ_C 124.0 (C-12) and 147.7 (C-13)], an oxymethine group [δ_H 4.18, 1H, dd, J = 9.0, 3.4 Hz; δ_C 77.5 (C-11)], and an oxygenated tertiary carbon signal [δ_C 77.3 (C-17)]. Two additional olefinic protons were located at C-1 (δ_H 7.87, 1H, d, J = 10.3 Hz; δ_C 164.5) and C-2 (δ_H 5.75, 1H, d, J = 10.3 Hz; δ_C 124.6) based on the HMBC correlations from H-1 (δ_H 7.87) to C-3 (δ_C 207.3) and C-10 (δ_C 41.8). The coupling constant of 9.0 Hz between H-9 and H-11 as well as the NOESY correlations indicated that compound **4** has the same HO-17β and MeO-11α orientations as those of **3**. Therefore, the structure of **4** was defined as 17β-hydroxy-11α-methoxy-3,16-dioxo-28-noroleana-1,12-diene.

https://dx.doi.org/10.1021/acs.jnatprod.9b00964
J. Nat. Prod. 2020, 83, 2076−2086

Table 1. ^{1}H NMR Spectroscopic Data for Compounds 1−6

	1[a]	2[c]	3[b]	4[b]	5[d]	6[d]
pos.	δ_H (J in Hz)	δ_H (J in Hz)	δ_H (J in Hz)	δ_H (J in Hz)	δ_H (J in Hz)	δ_H (J in Hz)
1	1.90, ddd (13.1, 7.4, 3.8)	3.88, t (6.9)	3.89, t (7.1)	7.87, d (10.3)	1.58, m	2.48, m
	1.49, m					1.64, m
2	2.54, m	2.76, dd (15.2, 7.7)	2.82, dd (15.2, 7.6)	5.75, d (10.3)	2.39, m	2.52, m
	2.33, ddd (15.9, 7.0, 3.8)	2.54, dd (15.2, 7.7)	2.44, dd (15.2, 7.6)		2.15, m	2.14, ddd (4.6, 10.6, 4.8)
5	1.44, m	1.30, m	1.41, m	1.65, m	2.24, m	1.56, m
6	1.55, m	1.61, m	1.61, m	1.64, m	1.94, m	1.68, m
		1.64, m	1.64, m		1.50, m	1.56, m
7	1.57, m	1.33, m	1.33, m	1.36, m	3.87, dd (11.2, 4.3)	3.79, br dd (10.8, 5.5)
	1.35, m	1.52, m	1.55, m	1.56, m		
9	1.70, dd (11.6, 6.4)	1.77, d (8.5)	1.98, d (8.9)	1.99, d (9.0)	1.68, dd (11.7, 5.6)	1.69, dd (11.7, 5.6)
11	2.07, m	4.34, dd (8.5, 3.7)	4.39, dd (9.0, 3.7)	4.18, dd (9.0, 3.4)	2.15, m	1.99, m
	2.02, m					2.08, m
12	5.43, t (3.6)	5.46, d (3.6)	5.58, d (3.7)	5.67, d (3.4)	5.48, br s	5.49, t (3.7)
15	3.32, d (13.1)	3.24, d (13.3)	3.26, d (13.4)	3.26, d (13.4)	3.56, d (14.3)	3.53, d (13.9)
	1.62, d (13.2)	1.70, d (13.3)	1.72, d (13.4)	1.70, d (13.4)	2.24, d (14.3)	2.24, d (13.9)
18	2.81, dd (14.2, 4.2)	2.83, dd (14.2, 4.2)	2.92, dd (14.3, 3.9)	2.87, dd (14.3, 3.9)	2.81, dd (14.3, 3.7)	2.81, dd (14.2, 4.2)
19	1.52, m	1.35, m	1.32, m	1.31, m	1.55, m	1.56, m
	1.26, m	1.38, m	1.46, m	1.46, m	1.29, m	1.26, m
21	1.62, m	1.30, m	1.30, m	1.29, m	1.63, m	1.61, m
	1.20, m	1.57, m	1.59, m	1.58, m	1.20, m	1.19, m
22	1.47, m	2.04, br d (13.4)	2.04, ddd (13.4, 4.1, 2.6)	2.04, ddd (13.3, 4.1, 2.6)	2.07, m	2.08, m
		1.45, br d (13.4)	1.45, ddd (13.4, 4.1, 2.6)	1.45, m	1.45, m	1.46, m
23	1.03, s	1.08, s	1.08, s	1.12, s	4.90, m	1.29, s
					4.72, m	
24	1.06, s	1.09, s	1.09, s	1.15, s	1.76, s	1.24, s
25	1.11, s	1.14, s	1.20, s	1.34, s	0.96, s	1.13, s
26	1.17, s	1.20, s	1.07, s	1.24, s	1.17, s	1.15, s
27	1.17, s	1.26, s	1.27, s	1.23, s	1.25, s	1.23, s
29	3.16, t (5.6)	0.89, s	1.01, s	1.01, s	3.15, d (2.3)	3.16, br dd (5.0, 2.5)
30	0.96, s	1.00, s	0.89, s	0.89, s	0.95, s	0.96, s
1′					3.59, s	3.99, t (6.7)
2′						1.53, m, 1.41, m
3′						1.59, m, 1.37, m
4′						0.91, t (7.4)
HO-4						3.28, s
HO-7						3.33, d (4.9)
HO-17	4.29, s					4.18, s
HO-29	3.57, t (5.6)					3.57, t (5.6)
MeO-11			3.34, s	3.38, s		

[a]Recorded in acetone-d_6 at 600 MHz. [b]Recorded in methanol-d_4 at 600 MHz. [c]Recorded in methanol-d_4 at 500 MHz. [d]Recorded in acetone-d_6 at 500 MHz.

Compound **5** was obtained as a white amorphous powder with $[\alpha]_D^{25}$ −3 (*c* 0.1, MeOH). Its positive ion HRESIMS data indicated the presence of an $[M + H - H_2O]^+$ ion at *m/z* 485.3260 (calcd for $C_{30}H_{45}O_5$, 485.3262), corresponding to the molecular formula $C_{30}H_{46}O_6$. Its IR spectrum showed the presence of hydroxy (3679 cm^{-1}), carbonyl (1713 cm^{-1}), and olefinic (1548 cm^{-1}) functionalities. Its ^{1}H NMR spectrum showed the presence of five methyl signals (δ_H 1.76, 1.25, 1.17, 0.96, and 0.95) as well as a methoxy group at δ_H 3.59, and of these, the methyl group at δ_H 1.76 was linked to a double bond, while the methoxy group was determined to be part of an ester. The two olefinic protons at δ_H 4.90 and 4.72 suggested an exocyclic double bond in addition to the endocyclic double bond (δ_H 5.48, 1H, br s). The spectra also suggested the presence of an oxymethine and a hydroxymethyl group based on the signals at δ_H 3.87 (J = 11.2, 4.3 Hz) and 3.15 (J = 2.3 Hz), respectively. The ^{13}C NMR data (Table 2) showed 30 carbon signals comprising two carbonyl carbons (δ_C 214.8, 174.4), two double bonds [one disubstituted double bond at δ_C 147.2 (C-4) and 114.5 (C-23) and a trisubstituted double bond at δ_C 142.5 (C-13) and δ_C 124.9 (C-12)], and three oxygenated carbons at δ_C 76.8 (C-17), 73.8 (C-29), and 72.1 (C-7). In the HMBC spectrum of **5**, the cross-peaks indicated the presence of a 3,4-*seco*-oleanane-type triterpenoid (Figure 1A) and the presence of a C-5 propenyl group based on a comparison with the spectrum of camelliaolean A.[14,16] Similar to compound **1**, the cross-peak from H_2-15 (δ_H 3.56, 2.24) to the carbonyl group at δ_C 214.8 defined the position of the carbonyl group at C-16. The three hydroxy groups were located at C-7, C-17, and C-29 by the correlations from H-5 (δ_H 2.24) and H_2-6 (δ_H 1.94, 1.50) to C-7, from H-18 (δ_H 2.81) to C-17, and from H_2-29 (δ_H 3.15) to

https://dx.doi.org/10.1021/acs.jnatprod.9b00964
J. Nat. Prod. 2020, 83, 2076−2086

Table 2. ^{13}C NMR Spectroscopic Data for Compounds 1−6

	1[a]	2[c]	3[b]	4[b]	5[d]	6[d]
pos.	δ_C	δ_C	δ_C	δ_C	δ_C	δ_C
1	39.6	79.1	78.9	164.5	34.6	35.1
2	34.5	43.8	43.2	124.6	28.7	29.4
3	216.0	217.5	217.9	207.3	174.4	174.8
4	47.8	48.0	49.0	45.9	147.2	75.0
5	55.8	52.1	51.8	54.2	48.4	50.0
6	20.2	19.9	19.9	19.9	35.7	34.1
7	33.2	33.9	33.9	34.3	72.1	72.8
8	40.5	44.9	45.0	44.9	45.5	45.7
9	46.8	55.6	50.3	47.7	38.2	39.4
10	37.5	44.9	45.1	41.8	40.1	42.1
11	24.3	67.3	75.8	77.5	24.4	24.1
12	124.4	127.5	123.9	124.0	124.9	125.5
13	143.0	146.0	149.6	147.7	142.5	142.2
14	48.7	49.0	49.0	49.0	50.0	50.1
15	43.3	44.0	44.0	43.8	46.8	46.9
16	213.9	215.8	215.5	215.6	214.8	214.8
17	77.2	77.4	77.3	77.3	76.8	76.9
18	52.6	52.8	53.3	53.2	53.0	53.1
19	43.2	48.2	48.4	48.4	43.1	43.1
20	36.6	31.6	31.7	31.7	36.6	36.6
21	32.2	37.7	37.7	37.7	32.1	32.2
22	30.8	31.5	31.4	31.4	30.6	30.7
23	26.9	27.1	27.5	28.2	114.5	33.9
24	21.8	21.5	21.3	22.1	23.8	28.4
25	15.3	12.4	12.6	20.2	20.1	20.4
26	17.7	19.1	19.3	19.9	11.0	10.9
27	27.1	26.9	26.0	26.5	26.8	26.6
29	73.9	32.9	32.9	32.9	73.8	74.0
30	19.4	23.9	23.9	23.9	19.4	19.4
1′					51.7	64.4
2′						31.6
3′						19.8
4′						14.0
MeO-11			49.0	54.8		

[a]Recorded in acetone-d_6 at 150 MHz. [b]Recorded in methanol-d_4 at 150 MHz. [c]Recorded in methanol-d_4 at 125 MHz. [d]Recorded in acetone- d_6 at 125 MHz.

C-20 (δ_C 36.6) and C-21 (δ_C 32.1). The position of the disubstituted double bond, which was connected to C-5 and the terminal methyl group (C-24), was determined based on the HMBC correlations from H_2-23 (δ_H 4.90, 4.72) to C-5 (δ_C 48.4) and C-24 (δ_C 23.8). The *seco*-A moiety of the oleanane skeleton of compound **5** was confirmed by the absence of an HMBC correlation between H_2-2 and C-4 and the presence of cross-peaks from the methoxy group (δ_H 3.59) and H_2-2 (δ_H 2.39, 2.15) to the ester carbonyl (δ_C 174.4). The relative configuration of compound **5** was determined through a NOESY experiment and a comparison of the coupling constants with camelliaolean B.[14] The coupling pattern of H-7 (dd, J = 11.2, 4.3 Hz) suggested the α-orientation of H-7, which was supported by the NOESY correlations from H-7 (δ_H 3.87) to H-5 and Me-27 (δ_H 1.25) (Figure 1B). In addition, the coupling constants of H-18 (dd, J = 14.3, 3.7 Hz), similar to those in **1**, suggested a β-orientation for H-18. The NOESY correlation between H-18 and Me-30 (0.96, s), shown in Figure 1B, also confirmed the β-orientation of Me-30. Therefore, the structure of compound **5** was defined as methyl 7β,17β,29-trihydroxy-16-oxo-3,4-*seco*-28-noroleana-4(23),12-dien-3-oate. It was confirmed that compound **5** is a natural product by comparison with the EtOAc-soluble fraction obtained from a 70% EtOH extract (Figure S43, Supporting Information).

Compound **6** was obtained as a white amorphous powder with $[\alpha]_D^{25}$ −10 (*c* 0.1, MeOH). Its negative ion HRESIMS data indicated an $[M + HCOO]^-$ ion at *m/z* 607.3848 (calcd for $C_{34}H_{55}O_9$, 607.3852), corresponding to the molecular formula $C_{34}H_{54}O_6$. Its IR spectrum showed the presence of hydroxy (3679 cm^{-1}), carbonyl (1713 cm^{-1}), and olefinic (1548 cm^{-1}) functionalities. The ^1H and ^{13}C NMR data (Tables 1 and 2) of **6** indicated that it is a 3,4-*seco*-oleanane triterpenoid similar to **5**. The difference between the NMR spectra of compounds **5** and **6** indicated the presence of an *n*-butoxy group in **6** instead of the methoxy group in **5**. In addition, there was an additional methyl group (δ_H 1.29, 3H, s; δ_C 33.9) and an oxygenated carbon (δ_C 75.0) in **6** instead of the C-5 propenyl group seen in **5**. The presence of the *n*-butoxy group was confirmed by the HMBC correlations (Figure 1A) from H_2-1′ (δ_H 3.99) and H_2-2 (δ_H 2.52, 2.14) to C-3 (δ_C 174.8), suggesting *n*-butyl esterification at C-3. The HMBC correlations from the protons of the two C-4 methyl groups at δ_H 1.29 and 1.24 and from the hydroxy proton (δ_H 3.28) to C-4 (δ_C 75.0) and C-5 (δ_C 50.0) suggested the C-5 propenyl group in **5** was replaced by a 2-hydroxyisopropyl group (Figure 1A). Similar to compound **5**, the α-orientation of H-7 was suggested by the coupling pattern of H-7 (br dd, J = 10.8, 5.5 Hz) and the NOESY correlations (Figure 1B) from H-7 (δ_H 3.79) to H-5 (δ_H 1.56) and Me-27 (δ_H 1.23). Furthermore, the β-orientation of Me-30 was identified based on the NOESY correlation between H-18 and Me-30 (0.96, s), as shown in Figure 1B. Thus, the structure of compound **6** was defined as *n*-butyl 4,7β,17β,29-tetrahydroxy-16-oxo-3,4-*seco*-28-norolean-12-en-3-oate. It was proven to be a natural product by the same method as for compound **5** (Figure S44, Supporting Information).

The neuroprotective effects of compounds **1**−**6** were investigated in a mouse hippocampal HT22 cell model. When cytotoxicity against a murine HT22 cell line was measured at a concentration of 40 μM, there was no measurable cytotoxicity (Figure S48, Supporting Information). The protective activities of compounds **1**−**6** in hippocampal HT22 cells against neuroinflammation induced by Aβ_{1-42} plasmid transfection were measured. As shown in Figure 2A, when the transfected-HT22 cells were treated with compounds **1**−**6** at a concentration of 40 μM, the neuroprotective effects of **1**−**4** were stronger than those of **5** and **6**. The protective effects of **1**−**4** were confirmed at different concentrations in the HT22 cell model transfected with the Aβ_{1-42} plasmids (Figures S49 and S50, Supporting Information). The antioxidant response element (ARE) transcriptional activity was significantly enhanced when HT22-ARE cells were transfected with the Aβ_{1-42} plasmids. When the cells were exposed to compounds **1**−**6** at a concentration of 40 μM, the increase in ARE gene transcriptional activity due to Aβ_{1-42} plasmid transfection was clearly reversed by cotreatment with compounds **1**−**4** (Figure 2B). As the Aβ_{1-42} plasmids contain the green fluorescent pEGFP-C1 gene, the intensity of the green fluorescence was measured after transfection with Aβ_{1-42} plasmids into the HT22 cells. Treatment with compounds **1**−**4** reduced the overexpression of the green fluorescent pEGFP-C1 gene (Figure 2C). Collectively, the data suggest that compounds **1**−**4** showed potential neuroprotective activity

https://dx.doi.org/10.1021/acs.jnatprod.9b00964
J. Nat. Prod. 2020, 83, 2076−2086

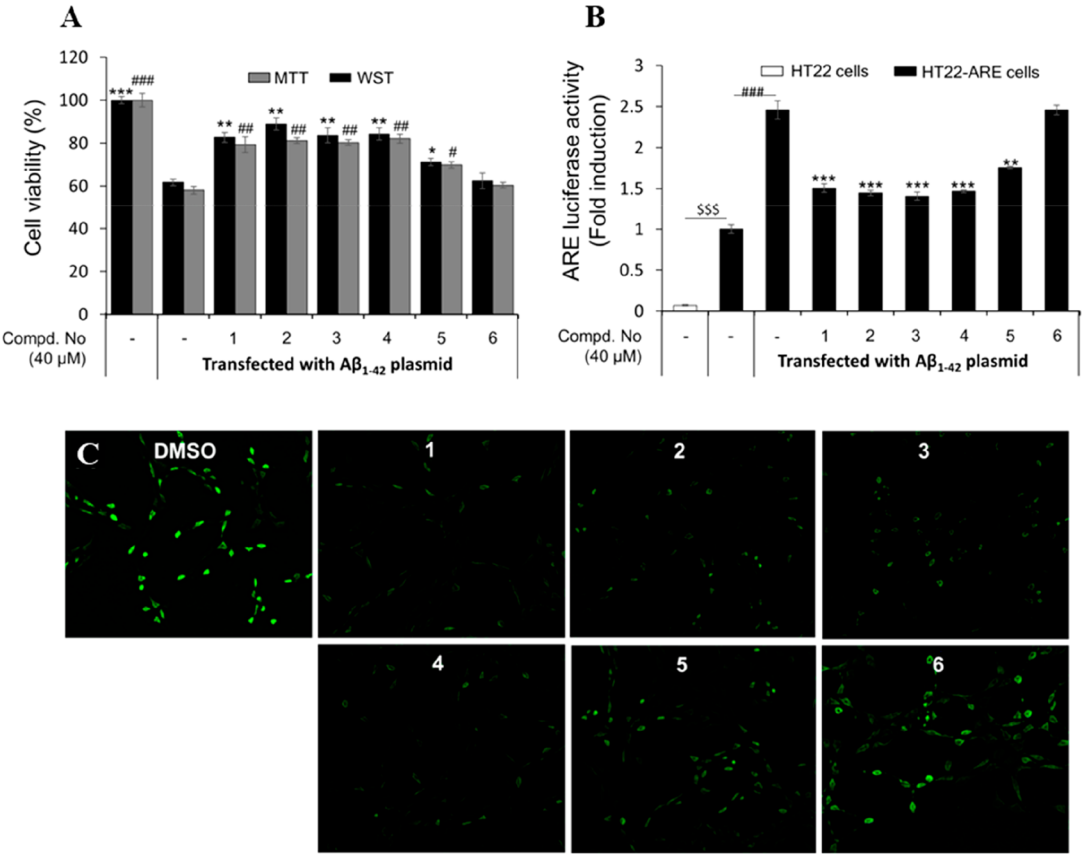

Figure 2. (A) Neuroprotective effects of compounds **1**−**6** against Aβ_{1-42} plasmid transfection in HT22 cells. After 10 h of transfection with the Aβ_{1-42} plasmids, the cells were treated with the test compounds at a concentration of 40 μM. The MTT and WST assays were performed after 1 day of incubation. Each value was calculated as the means ± SD (n = 3). For the MTT assay: $^{*}p < 0.05$, $^{**}p < 0.01$, $^{***}p < 0.001$ compared with the Aβ_{1-42} transfection untreated group. For the WST assay: $^{\#}p < 0.05$, $^{\#\#}p < 0.01$, $^{\#\#\#}p < 0.001$ compared with the Aβ_{1-42} transfection untreated group. (B) Effects of compounds **1**−**6** on ARE gene transcriptional activation. The transfected HT22-ARE cells were treated with the test compounds at a concentration of 40 μM. The ARE transcriptional activity was measured using a luciferase assay kit. Data were calculated as the means ± SD (n = 3). Significance was accepted at $^{\$\$\$}p < 0.001$ HT22-ARE cells compared with the HT22 cell group; $^{\#\#\#}p < 0.001$ compared with the nontransfection group; $^{**}p < 0.01$ and $^{***}p < 0.001$ compared with the Aβ_{1-42} transfection untreated group. (C) Effects of triterpenoids **1**−**6** on the intensity of the green fluorescence induced by pEGFP-C1/Aβ_{1-42} plasmid transfection in the HT22 cell line. The cells were transfected with Aβ_{1-42} plasmids using Lipofectamine for 10 h. The transfected cells were continually exposed to the test compounds at a concentration of 40 μM. After 24 h of incubation, the cells were visualized using fluorescence microscopy.

against neuroinflammation induced by Aβ_{1-42} plasmid transfection in hippocampal HT22 cells.

The Aβ hypothesis proposes a link between the pathophysiology of AD with amyloid precursor protein (APP), which is cleaved by α-, β-, and γ-secretases. In the brain, β-secretase 1 (BACE1) is the main component of β-secretase, and cleavage by BACE1 is the rate-limiting step in Aβ generation. Thus, BACE1 has been suggested as a potential target for the treatment of early-stage AD.[17] To clarify the relationship between the neuroprotective effects of compounds **1**−**6** from *C. japonica* and their Aβ inhibitory effects, their BACE1 enzyme activities and docking simulation studies on BACE1 were assessed. Compounds **1**−**4** (20 μM) showed inhibitory activities of approximately 60.56, 51.08, 51.89, and 61.29%, respectively, on enzyme activity of BACE1 (Figure S51, Supporting Information). Compounds **1**−**4** also showed inhibitory effects on BACE1 at different concentrations (10 and 20 μM) compared to quercetin (10 μM), which was used as a positive control. In conjunction with the results of previous studies on the in vitro inhibitory activities of triterpenoids on BACE1, these results suggest that triterpenoids from *C. japonica* have potential as anti-AD inhibitory materials by inhibiting BACE1 (Figure 3A).[18−20] Thus, to further understand the pharmacological effects of triterpenoids from *C. japonica* on the prevention of cell death caused by glutamate- or Aβ_{1-42}-transfected HT22 cells, molecular docking simulation studies involving BACE1 (PDB ID: 2WJO) and compounds **1**−**4** were conducted using the CDOCKER protocol in CHARMM force fields. The interactions between this protein and the small molecules through hydrogen bonds, van der Waals interactions, alkyl, and pi-alkyl interactions are shown in Figures 3B,C, Figures S52−S55, and Table S1 (Supporting Information). The CDOCKER interaction energies of compounds **1**−**4**, which were obtained from molecular docking simulations, were calculated to be −39.30, −45.35, −45.24, and −41.97 kcal/mol, respectively (Table S1, Supporting Information). Interestingly, comparing our results to those of previous studies indicated that the key amino acids, including Asp32, Gly230, Ile118, and Tyr71, responsible for the interactions of these four new triterpenoids (**1**−**4**) with BACE1 were the same.[18,20] These *in silico* docking results provide a new natural product platform for the preparation of AD therapeutics via BACE1 blockade.

https://dx.doi.org/10.1021/acs.jnatprod.9b00964
J. Nat. Prod. 2020, 83, 2076−2086

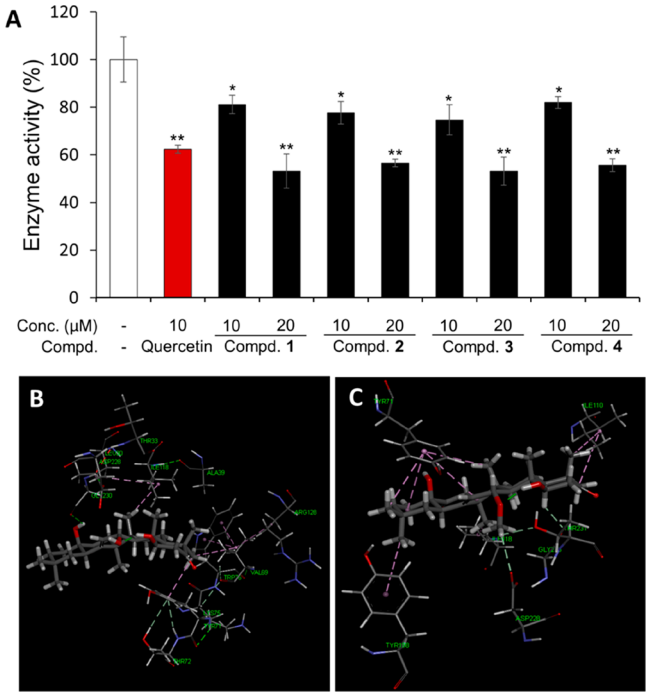

Figure 3. BACE1 inhibitory activity of isolated compounds **1**−**4** from *C. japonica* at different concentrations (A). Data are presented as means ± SD (n = 3). Significance was accepted at *p < 0.05, **p < 0.01 compared with the positive control. 3D docking simulation of BACE1 (PDB ID: 2WJO) with compounds **2** (B) and **3** (C).

In the pathophysiology of AD, extracellular Aβ has been reported to block neuronal glutamate uptake at the synapses and increase the amount of glutamate in the synaptic cleft.[21] Recent studies indicated that nanomolar concentrations of Aβ can enhance glutamate release in hippocampal neurons.[22−24] However, the effects of extracellular Aβ on glutamate release/uptake remain controversial.[22,25,26] In this study, the changes in glutamate levels in HT22 cells transfected with the Aβ_{1-42} plasmids in the presence or absence of the test compounds were evaluated. As shown in Figure 4A, the glutamate level of HT22 cells transfected with Aβ_{1-42} was significantly increased compared to that of nontransfected cells. This result suggested that HT22 cells transfected with Aβ_{1-42} plasmids would show increased expression of Aβ_{1-42} protein after incubation and would have damaged glutamate transporters, leading to the blockage of glutamate uptake. Because of the cytotoxicity of Aβ_{1-42} protein in HT22 cells transfected with Aβ_{1-42}, we could not increase the incubation time. When we measured the intracellular glutamate level after 24 h of incubation, the glutamate level was increased by approximately 3.17-fold in HT22 cells transfected with Aβ_{1-42}. Interestingly, compounds **1**−**4** at a concentration of 40 μM clearly reduced glutamate levels by approximately 1.81-, 1.42-, 1.61-, and 1.80-fold, respectively (Figure 4A). This result suggested that **1**−**4** decreased glutamate levels in HT22 cells transfected with Aβ_{1-42}. Thus, the protective effects of compounds **1**−**4** against glutamate-induced cytotoxicity were further confirmed. Glutamate, a major excitatory neurotransmitter in the CNS of mammals, is known to be involved in many chronic brain diseases.[22,27−29] HT22 cell lines have been used as a good model for glutamate-induced neurotoxicity.[30,31] In this study, the neuroprotective effects of compounds **1**−**6** at a concentration of 40 μM against glutamate-induced neurotoxicity in HT22 cells were studied. Figure 4B shows that compounds **1**−**4** exhibited protective effects against treatment with glutamate (10 mM) in HT22 cells that were 81.2, 78.1, 77.0, and 73.8%, respectively, stronger than that of the untreated control. Collectively, these results strongly suggested that triterpenoids exhibit neuroprotective action to reduce glutamate levels and prevent glutamate-induced cytotoxic symptoms in AD. Therefore, these results indicate that the biological mechanisms of active triterpenoids **1**−**4** are worthy of further study.

As mentioned above, the accumulation of Aβ in the AD brain increases pro-inflammatory cytokines and neurotoxic compounds such as NO, resulting in neuroinflammation in microglial cells. The cytotoxicities of triterpenoids **1**−**6** were examined in murine BV2 microglial cells before the effects of these compounds against NO production were evaluated in Aβ_{1-42}-transfected microglial cells. As shown in Figures S56 and S57 (Supporting Information), compounds **1**−**6** did not affect cell viability. Thus, we evaluated their inhibitory effect on NO production in Aβ_{1-42}-transfected BV2 microglial cells to demonstrate their anti-neuroinflammatory activity. As shown in Figure 4C, compounds **1**−**4** decreased NO production in Aβ_{1-42}-transfected BV2 cells. This reduction in NO production was further examined in a concentration-dependent manner over a concentration range of 10 to 40 μM (Figure 4D). The decrease in NO production by NO-enhanced Aβ_{1-42}-transfected BV2 microglial cells upon treatment with compounds **1**−**4** provided additional evidence of a neuroprotective effect against Aβ-induced neuroinflammation, which is part of the pathophysiology of AD.

The 24 known compounds isolated from *C. japonica* provided by the KBNMB and six new compounds (**1**−**6**) (Figure S58, Supporting Information) were evaluated for SARs in a model of Aβ_{1-42}-transfected HT22 cells. Cytotoxicity data (Figure S59, Supporting Information) showed that several compounds significantly reduced the cell viability at a concentration of 40 μM. According to this result, the isolated compounds from *C. japonica* could be classified into three groups for further confirming the neuroprotective effect against Aβ-induced cytotoxicity at different concentrations: (group 1) CPP1033, 1041, 1042, 1043, 1045, 1051, 1053, 1054, 1063, 1070, 1073, and 1074; (group 2) CPP1032, 1037, 1038, 1067, 1210, and 1211; (group 3) CPP1031, 1035, 1036, 1040, 1055, and 1069. As shown in Figure S60 (Supporting Information), after treatment with 20 μM (group 1), 5 μM (group 2), and 1 μM (group 3) for 24 h, the viability of Aβ_{1-42}-transfected HT22 cells substantially increased to 68.9−75.2% relative to the Aβ_{1-42}-transfected control value (51.2%) with CPP1032, 1037, 1051, and 1054. Based on the bioactivity data in Figures 2A and S60 (Supporting Information), the preliminary SARs of triterpenoids from *C. japonica* were analyzed as follows: (a) HO-17 and C-16 carbonyl groups on a basic β-amyrin skeleton were crucial for the neuroprotective activity (**1**−**4**, CPP1032 and 1051). In addition, compounds with four monosaccharide units (CPP1210 and 1211) or ethyl glucuronate (CPP1069) or without any substituent (CPP1031) on C-3 displayed less potent activity than CPP1032 and 1051. In particular, the C-3 carbonyl group was important for anti-Aβ_{1-42} activity (**2**−**4**). Moreover, replacement of the hydroxy group on the C-29 position (**1**) with hydrogen (CPP1033) showed diminished neuroprotective activity and induced cytotoxicity. (b) The activity of CPP1054 was substantially increased to 72.0% compared with CPP1036, 1040, 1053, 1055, 1063, and 1067

https://dx.doi.org/10.1021/acs.jnatprod.9b00964
J. Nat. Prod. 2020, 83, 2076−2086

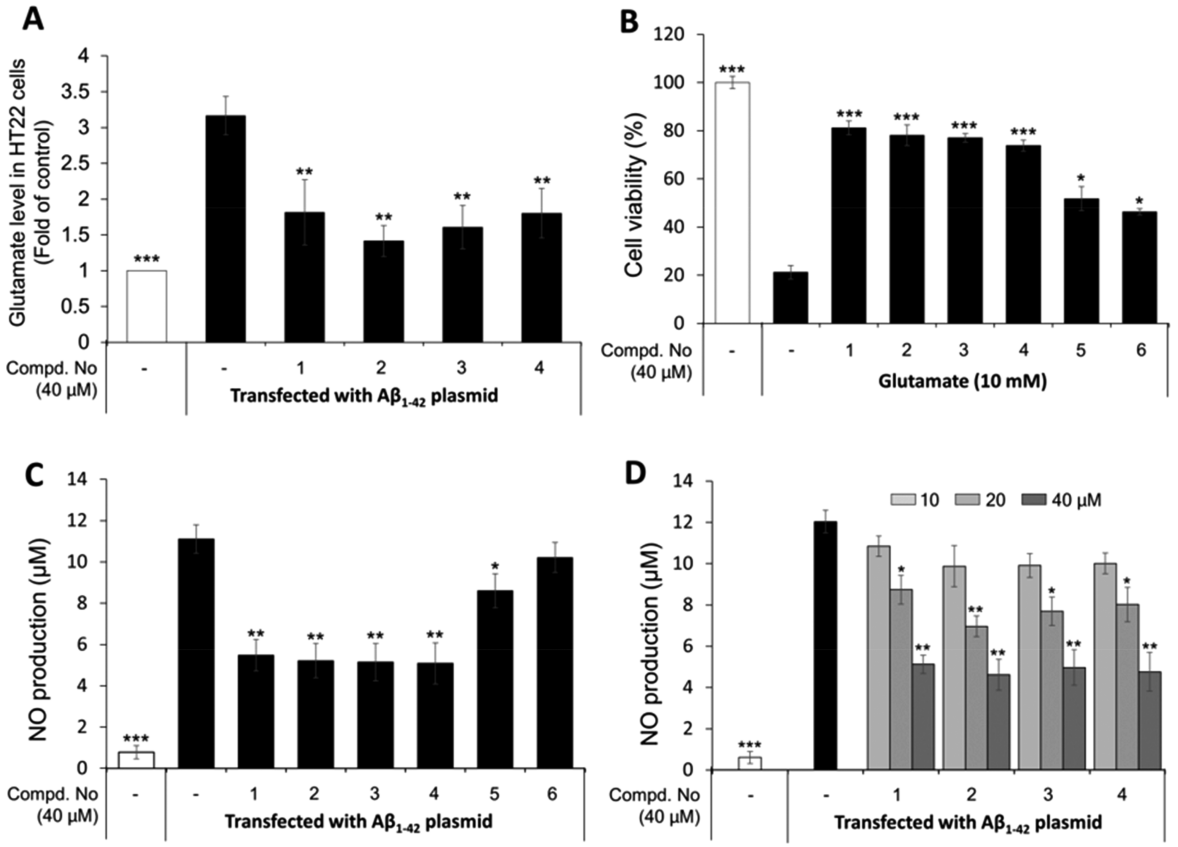

Figure 4. (A) Comparison of the intracellular glutamate concentration in HT22 cells under different conditions: nontransfected, Aβ_{1-42} plasmid-transfected without treatment, and Aβ_{1-42} plasmid-transfected with treatment with compounds **1**−**4** at a concentration of 40 μM. The results are presented as the means ± SD of four independent experiments. Significance was accepted at $^{*}p < 0.05$, $^{**}p < 0.01$, and $^{***}p < 0.001$ compared with the Aβ_{1-42} transfection untreated control. (B) Neuroprotective effects of compounds **1**−**6** against glutamate-induced toxicity using HT22 cells. After 16 h of incubation with the test compounds at a concentration of 40 μM, the cell viability was evaluated using the MTT method. Data are expressed as the means ± SD ($n = 3$); $^{*}p < 0.05$, $^{***}p < 0.001$ compared with glutamate treatment only. Inhibitory effects of compounds **1**−**6** on NO production in Aβ_{1-42}-transfected BV2 microglial cells. BV2 cells were transfected with Aβ_{1-42} plasmids using Lipofectamine for 10 h. The transfected cells were then treated with the test compounds at a concentration of 40 μM (C) or compounds **1**−**4** at different concentrations (D). After 18 h of incubation, the NO production was evaluated by the Griess method. Data were calculated as the means ± SD ($n = 3$); $^{*}p < 0.05$, $^{**}p < 0.01$, $^{***}p < 0.001$ compared with the Aβ_{1-42} transfection untreated group.

(56.3, 61.9, 55.5, 60.5, 61.7, and 58.6%, respectively). These results indicated that different substituents on the C-3 position in combination with HO-16 and C-17 carboxyl groups showed important features for the neuroprotective effect. (c) Notably, 3,4-*seco*-noroleanane-type species (**5**, **6**, CPP1041, 1043, 1045, 1073, 1070, and 1074) failed to show any potent activity against Aβ_{1-42}-induced cytotoxicity. The poor activity of these compounds indicated that the anti-Aβ_{1-42} activities of triterpenoids were significantly related to the noroleanane skeleton, whereas the *seco*-noroleanane series could be promising neuroprotective agents against Parkinson's disease.[12] The pharmacokinetics and mechanism of these kinds of triterpenoids require further studies.

In conclusion, four out of the six new compounds, **1**−**4**, showed strong neuroprotective effects against Aβ- and glutamate-induced cytotoxicity. Treatment of Aβ_{1-42}-transfected HT22 cells with compounds **1**−**4** reduced intracellular glutamate levels, increased cell viability, and inhibited BACE1. Moreover, molecular docking simulations on BCAE1 with these noroleananes provide additional persuasive evidence supporting the aforementioned results of **1**−**4**. In addition, treatment with compounds **1**−**4** inhibited NO production, demonstrating their strong anti-neuroinflammatory activity in BV2 cells transfected with Aβ_{1-42}. The results strongly suggest that new noroleanane-type triterpenoids **1**−**4** are potential candidates for further studies on AD treatment.

■ EXPERIMENTAL SECTION

General Experimental Procedures. Optical rotations were measured on a JASCO P-2000 polarimeter (JASCO International Co. Ltd., Tokyo, Japan) with a 10 mm path length cell. The UV spectra were measured on a Chirascan-Plus CD spectrometer (Applied Photophysics, Leatherhead, UK). The IR spectra were recorded on an FT/IR-4200 FT-IR spectrometer (Thermo Electron Corp., Waltham, MA, USA). NMR spectra were obtained using AVANCE-500 (Bruker, Rheinstetten, Germany) and JNM-ECA-600 MHz (JEOL, Tokyo, Japan) spectrometers at the College of Pharmacy, Seoul National University, Republic of Korea. The HRESIMS data were obtained using an Agilent 6530 qTOF spectrometer (Agilent Technologies, Santa Clara, CA, USA) accompanied by ESIMS spectra, which were obtained on an Agilent 1100 series LC/MSD TRAP spectrometer (Agilent Technologies, Waldbronn, Germany) and a Waters Xevo G2 QTOF mass spectrometer (Waters Co., Milford, MA, USA). Column chromatography (CC) separations were carried out using silica gel (63−200 μm particle size, Merck, Germany) and RP-C_{18} (40−63 μm particle size, Merck, Germany). Silica gel 60 F_{254} and RP-18 F_{254} plates were used for analytical TLC separations (Merck, Darmstadt, Germany). A

https://dx.doi.org/10.1021/acs.jnatprod.9b00964
J. Nat. Prod. 2020, 83, 2076−2086

Gilson preparative high-performance liquid chromatography (HPLC) system was used for the purification of individual natural compounds, and the system was equipped with a 321 pump and a UV/vis-155 detector. An Optima Pak C_{18} column (10 × 250 mm, 10 μm particle size, RS Tech, Seoul, Korea) was used for the HPLC separation. All solvents used for extraction and isolation were of analytical grade.

Plant Material. *C. japonica* fruit peels were collected from Jeju Island in 2011 and authenticated by Prof. W. K. Oh. A voucher specimen (SNU2011-11) was deposited at the KBNMB, Research Institute of Pharmaceutical Sciences, College of Pharmacy, Seoul National University, Seoul, Republic of Korea.

Extraction and Isolation. The dried fruit peels of *C. japonica* (7 kg) were powdered and extracted at room temperature by sonication with MeOH (3 × 10 L, each 3 h). The MeOH extract was dried under reduced pressure, and the residue was suspended in water and partitioned successively into *n*-hexane, EtOAc, and *n*-BuOH. The EtOAc-soluble part (50.0 g) was chromatographed over silica gel eluted with an *n*-hexane/acetone gradient (9:1 to 1:9, v/v) to yield five fractions (F1−F5). Fraction F4 (5.6 g) was applied to an RP-C_{18} column and eluted with a MeOH/H_2O gradient (1:1 to 10:1, v/v) to afford six subfractions (F4.1−F4.6). F4.6 (1.2 g) was separated on a silica gel column using a CH_2Cl_2/MeOH gradient (40:1 to 1:1) to obtain four subfractions (F4.6.1−F4.6.4). F4.6.2 (0.4 g) was repeatedly separated by normal silica gel CC eluting with gradient mixtures of *n*-hexane/acetone (5:1 to 1:1) to yield three subfractions (F4.6.2.1−F4.6.2.3). F4.6.2.2 (50 mg) was purified by prep-HPLC on an Optima Pak C_{18} column [the elution system was composed of H_2O containing 0.1% formic acid (A) and MeOH (B): 0−25 min: 62% B/A, 25−27 min: 62 to 68% B/A gradient, 27−60 min: 68% B/A, 60−62 min: 68 to 100% B/A gradient, 62−70 min: 100% B; flow rate: 2 mL/min; UV detection at 205 and 254 nm] to give compound **1** (3.26 mg, t_R = 55 min). F4.6.3 (0.5 g) was repeatedly separated by silica gel CC with an *n*-hexane/acetone gradient (8:1 to 1:1) to yield three subfractions (F4.6.3.1−F4.6.3.3). F4.6.3.2 (60 mg) was separated by prep-HPLC [the elution system was composed of H_2O containing 0.1% formic acid (A) and MeCN (B); 0−60 min: 42% B/A, 60−62 min: 42 to 100% B/A gradient, 62−70 min: 100% B; flow rate: 2 mL/min; UV detection at 205 and 254 nm] to afford compound **5** (2.2 mg, t_R = 48 min). F4.6.4 (0.6 g) was repeatedly separated by normal silica gel CC with gradient elution (*n*-hexane/acetone, 5:1 to 1:1) to yield two subfractions (F4.6.4.1 and F4.6.4.2). F4.6.4.2 (53 mg) was further purified by prep-HPLC [the elution system was composed of water containing 0.1% formic acid (A) and MeOH (B); 0−45 min: 68% B/A, 45−47 min: 68 to 100% B/A gradient, 47−55 min: 100% B; flow rate: 2 mL/min; UV detection at 205 and 254 nm] to provide compound **6** (3.0 mg, t_R = 38 min).

The *n*-BuOH-soluble part was chromatographed over silica gel eluting with an EtOAc/MeOH gradient (20:1 to 1:1) to yield eight fractions (FB1−FB8) based on the TLC profile. Fraction FB1 (10 g) was applied to an RP-C_{18} column and eluted with a MeOH/H_2O gradient (1:1 to 10:1) to afford 10 subfractions (FB1.1−FB1.10). Fraction FB1.8 (1.5 g) was applied to an RP-C_{18} column and eluted with a MeOH/H_2O gradient (4:6 to 10:1) to afford eight subfractions (FB1.8.1−FB1.8.8). FB1.8.1 (50 mg) was purified by prep-HPLC [the elution system was composed of water containing 0.1% formic acid (A) and MeOH (B); 0−45 min: 58% B/A, 45−47 min: 58 to 100% B/A gradient, 47−55 min: 100% B; flow rate: 2 mL/min; UV detection at 205 and 254 nm] to afford compound **2** (2.0 mg, t_R = 32 min). FB1.8.2 (0.2 g) was purified by prep-HPLC [the mobile phase consisted of H_2O containing 0.1% formic acid (A) and MeOH (B); 0−47 min: 58% B/A, 47−55 min: 100% B; flow rate: 2 mL/min; UV detection at 205 and 254 nm] to give compound **3** (5.0 mg, t_R = 25 min). FB1.8.3 (0.3 g) was purified by prep-HPLC using H_2O with 0.1% formic acid (A) and MeOH (B) (0−45 min: 50% B/A, 45−47 min: 50 to 100% B/A gradient, 47−55 min: 100% B; flow rate: 2 mL/min; UV detection at 205 and 254 nm) to afford compound **4** (6.0 mg, t_R = 25 min).

17β,29-Dihydroxy-3,16-dioxo-28-norolean-12-ene (**1**): amorphous powder; $[\alpha]_D^{25}$ −29 (*c* 0.1, MeOH); IR ν_{max} 3415, 2941, 1702, 1457, 1385, 1246, 1204, 1114, 1029, 1003 cm^{-1}; UV (MeOH) λ_{max} (log ε) 218 (2.60) nm; ^1H and ^{13}C NMR data, see Tables 1 and 2; HRESIMS *m/z* 439.3209 $[M + H - H_2O]^+$ (calcd for $C_{29}H_{43}O_3$, 439.3207).

1β,11α,17β-Trihydroxy-3,16-dioxo-28-norolean-12-ene (**2**): amorphous powder; $[\alpha]_D^{25}$ −15 (*c* 0.1, MeOH); IR ν_{max} 3392, 2926, 2853, 2349, 2310, 1713, 1461, 1386, 1243 cm^{-1}; UV (MeOH) λ_{max} (log ε) 218 (2.59) nm; ^1H and ^{13}C NMR data, see Tables 1 and 2; HRESIMS *m/z* 473.3274 $[M + H]^+$ (calcd for $C_{29}H_{45}O_5$, 473.3267).

1β,17β-Dihydroxy-11α-methoxy-3,16-dioxo-28-norolean-12-ene (**3**): amorphous powder; $[\alpha]_D^{25}$ −40 (*c* 0.1, MeOH); IR ν_{max} 3566, 2924, 2852, 2372, 2320, 1744, 1595, 1509, 1466, 1339 cm^{-1}; UV (MeOH) λ_{max} (log ε) 210 (2.74) nm; ^1H and ^{13}C NMR data, see Tables 1 and 2; HRESIMS *m/z* 509.3198 $[M + Na]^+$ (calcd for $C_{30}H_{46}NaO_5$, 509.3237).

17β-Hydroxy-11α-methoxy-3,16-dioxo-28-noroleana-1,12-diene (**4**): amorphous powder; $[\alpha]_D^{25}$ +21 (*c* 0.1, MeOH); IR ν_{max} 3382, 3725, 3586, 3565, 2924, 2852, 2359, 2309, 1748, 1596, 1508, 1386, 1338 cm^{-1}; UV (MeOH) λ_{max} (log ε) 210 (2.74) nm; ^1H and ^{13}C NMR data, see Tables 1 and 2; HRESIMS *m/z* 513.3223 $[M + HCOO]^-$ (calcd for $C_{31}H_{45}O_6$, 513.3222).

Methyl 7β,17β,29-trihydroxy-16-oxo-3,4-seco-28-noroleana-4(23),12-dien-3-oate (**5**): amorphous powder; $[\alpha]_D^{25}$ −3 (*c* 0.1, MeOH); IR ν_{max} 3679, 2947, 2865, 2844, 1713, 1548, 1455, 1347, 1304, 1249, 1198, 1176, 1126, 1096, 1052, 1032, 1019 cm^{-1}; UV (MeOH) λ_{max} (log ε) 215 (2.76) nm; ^1H and ^{13}C NMR data, see Tables 1 and 2; HRESIMS *m/z* 485.3260 $[M + H - H_2O]^+$ (calcd for $C_{30}H_{45}O_5$, 485.3262).

n-Butyl 4,7β,17β,29-tetrahydroxy-16-oxo-3,4-seco-28-norolean-12-en-3-oate (**6**): amorphous powder; $[\alpha]_D^{25}$ −10 (*c* 0.1, MeOH); IR ν_{max} 3694, 3679, 3392, 2949, 2865, 2843, 1706, 1455, 1388, 1346, 1187, 1112, 1052, 1032, 1018 cm^{-1}; UV (MeOH) λ_{max} (log ε) 212 (2.74) nm; ^1H and ^{13}C NMR data, see Tables 1 and 2; HRESIMS *m/z* 607.3848 $[M + HCOO]^-$ (calcd for $C_{34}H_{55}O_9$, 607.3852).

Cell Cytotoxicity and Transfection of the Aβ_{1-42} Gene into HT22 Cells. The cytotoxicity assay was performed using 3-[4,5-dimethylthiazol-2-yl]-2,5-diphenyl tetrazolium bromide (MTT) (Sigma, MO, USA). Briefly, the Aβ_{1-42} plasmids were kindly gifted to us by Professor Junsoo Park (Yonsei University, Korea).[2] HT22 cells were seeded into 96-well plates at 4000 cells/well in Dulbecco's modified Eagle's medium (DMEM) supplemented with 10% fetal bovine serum (FBS), 100 U/mL penicillin, and 100 μg/mL streptomycin, and the cells were incubated at 37 °C under 5% CO_2 for 2−3 h. The cells were transfected with 0.2 μg of Aβ_{1-42} plasmids in each well using Lipofectamine 2000 (Invitrogen, Carlsbad, CA, USA). After 10 h of incubation, the medium was replaced with fresh medium containing 2% FBS with or without the test compounds. The cultures were incubated for 24 h at 37 °C in a 5% CO_2 atmosphere. Then, 20 μL of MTT solution (2 mg/mL) was added to each well, and the cells were incubated in the dark for 4 h. The cell supernatants were removed, and DMSO was added to dissolve the formazan crystals. The absorbance was measured at 550 nm using a microplate reader (VersaMax, PA, USA). To measure the cell viability using the WST-1 cell proliferation reagent, 10 μL of this reagent was added to each well, and the cells were incubated for 2 h. The absorbance was then measured at 440 nm. The error bars indicate the mean ± SD of three independent experiments.

ARE-Reporter Gene Assay. HT22-ARE cells with the pGL4.37-[luc2P/ARE/Hyg] vector were subcultured in DMEM containing 10% FBS and 0.2 mM hygromycin.[2] The cells were seeded into 12-well plates at 2 × 10^5 cells per well and transfected with 5 μg of the Aβ_{1-42} plasmids using Lipofectamine 2000 for 10 h. The cells were transferred to a new medium supplemented with 1% FBS and treated with the test compounds for 18 h. The cell lysates were collected by adding 200 μL of passive lysis buffer (Promega, Madison, WI, USA). The cell lysates were incubated for 30 min and centrifuged at 12,000 rpm for 2 min. The amounts of protein in the supernatants were measured using the BCA protein assay kit (Bio-Rad Laboratories, CA, USA). The ARE-luciferase activity was measured using a dual-luciferase assay kit (Promega, Madison, WI, USA) and a luminescence microplate reader (SpectraMax, Molecular Devices, CA, USA).

https://dx.doi.org/10.1021/acs.jnatprod.9b00964
J. Nat. Prod. 2020, 83, 2076−2086

Nitrite Assay. Mouse microglial BV2 cells were seeded into 48-well plates at 5×10^4 cells/well. The cells were transfected with 1 μg of the Aβ_{1-42} plasmids using Lipofectamine 2000 for 10 h. After being replaced with a fresh phenol red-free medium, the cells were exposed to the test compounds for 18 h. The NO production was measured using the Griess method.[32]

Measurement of Glutamate after Transfection of the Aβ_{1-42} Gene into HT22 Cells. HT22 cells were grown in 60 mm culture dishes using DMEM supplemented with 10% FBS, 100 U/mL penicillin, and 100 μg/mL streptomycin. The cells were transfected with 10 μg of Aβ_{1-42} plasmids using Lipofectamine 2000 for 10 h. The medium was replaced with fresh medium containing 2% FBS with or without the test compounds. The cultures were incubated at 37 °C under 5% CO_2 for 24 h. Then, the cells were washed with PBS and collected. All samples were weighed and adjusted to a concentration of 20 mg/mL. In this assay, 50% MeOH in H_2O was used to dissolve the glutamate in the cell lysates and was used to prepare a solution of L-monosodium glutamate monohydrate (MSG) (Sigma, MO, USA) as a standard. The glutamate measurement was conducted based on the well-established reaction with *o*-phthalaldehyde (OPA) with several modifications.[33,34] For accurate quantitation, a standard curve was prepared with MSG at various concentrations. Based on the standard curve, for which $R^2 = 0.9936$, the glutamate in the cell lysates was measured in four independent experiments. The HPLC system consisted of an Agilent Series 1260 Infinity liquid chromatograph equipped with a G1322A vacuum degasser, a G1312C binary pump, a G1329B autosampler, a G1315D DAD, and an RF-10AXL fluorescence detector connected to Agilent ChemStation software (Agilent, Waldbronn, Germany). The ESIMS data were obtained using an Agilent Technologies 6130 qTOF MS/MS spectrometer (Agilent Technologies, Inc., Santa Clara, CA, USA). A reversed-phase INNO C_{18} column (4.6 × 150 mm, 5 μm, Young Jin Biochrom, Korea) was used for the separation of the reaction products. The flow rate was 0.6 mL/min from 0−33 min and 1 mL/min from 33−43 min. The mobile phase comprised 0.1% formic acid in MeCN (A) and 0.1% formic acid in H_2O (B). The gradient profile was as follows: 0−8 min: isocratic A:B (25:75); 8−18 min: gradient A:B (from 25:75 to 40:60); 18−23 min: gradient A:B (40:60−60:40); 23−33 min: gradient A:B (60:40−80:20); 33−40 min: gradient A:B (80:20−100:0); and 40−43 min, stepwise return to initial condition of A:B (25:75); flow rate: 0.3 mL/min. The injection volume was 20 μL. The raw LC/MS data are shown in Figures S61−S67 (Supporting Information).

Glutamate-Induced Neurotoxicity. HT22 cells were used for the glutamate-induced neurotoxicity studies.[30,31] The cells were seeded into 96-well plates at 5×10^3 cells/well using DMEM supplemented with 10% FBS, 100 U/mL penicillin, and 100 μg/mL streptomycin. After 6 h of incubation, the cells were exposed to 1% FBS medium containing glutamate (10 mM) in the presence or absence of the test compounds. After the cultures were incubated for 16 h at 37 °C under 5% CO_2, the MTT assay was carried out as described above.

In Vitro BACE1 Assay and Molecular Docking Simulation. The BACE1 is considered a rate-limiting factor in the production of Aβ in AD pathogenesis.[17,18] In this study, the BACE1 assay was performed using the BACE1 FRET assay kit (PanVera Co., Madison, WI, USA) with slight modifications, and quercetin was used as the positive control. Molecular docking between BACE1 and compounds (**1**−**4**) was simulated using the Discovery Studio 4.0/CDOCKER software (Accelrys, San Diego, CA, USA). The structure of BACE1 was obtained from the Protein Data Bank (http://www.pdb.org) with ID code 2WJO. The protein−ligand binding affinities were predicted using CDOCKER interaction energies. These interactions included conventional hydrogen bonds and carbon−hydrogen bonds as well as pi-alkyl, alkyl, and van der Waals interactions.

Statistical Analysis. Data were calculated and expressed as the means ± SD of three independent experiments. The mean values of different groups were compared using analysis of variance (ANOVA), which was carried out using SPSS Statistics 23 (SPSS, Inc., Chicago, IL, USA). Statistically significant p values were established at $^*p < 0.05$, $^{**}p < 0.01$, and $^{***}p < 0.001$.

■ ASSOCIATED CONTENT

Supporting Information

The Supporting Information is available free of charge at https://pubs.acs.org/doi/10.1021/acs.jnatprod.9b00964.

HRESIMS, 1D and 2D NMR, and infrared absorption spectra of new compounds **1**−**6**, cytotoxicity assay, MTT assay, WST assay, fluorescent and BACE1 inhibition assay results, docking simulation of BACE1 with compounds **1**−**4**, LC-MS profiles of the MSG-OPA product and the cell lysates-OPA product, CDOCKER protocol for molecular docking simulation of BACE1 (PDF)

■ AUTHOR INFORMATION

Corresponding Author

Won-Keun Oh − *Korea Bioactive Natural Material Bank, Research Institute of Pharmaceutical Sciences, College of Pharmacy, Seoul National University, Seoul 08826, Republic of Korea;* orcid.org/0000-0003-0761-3064; Phone: +82-02-880-7872; Email: wkoh1@snu.ac.kr

Authors

Hyo-Moon Cho − *Korea Bioactive Natural Material Bank, Research Institute of Pharmaceutical Sciences, College of Pharmacy, Seoul National University, Seoul 08826, Republic of Korea*

Thi-Kim-Quy Ha − *Korea Bioactive Natural Material Bank, Research Institute of Pharmaceutical Sciences, College of Pharmacy, Seoul National University, Seoul 08826, Republic of Korea; College of Natural Sciences, Cantho University, Cantho City, Vietnam*

Thi-Phuong Doan − *Korea Bioactive Natural Material Bank, Research Institute of Pharmaceutical Sciences, College of Pharmacy, Seoul National University, Seoul 08826, Republic of Korea*

Basanta Dhodary − *Korea Bioactive Natural Material Bank, Research Institute of Pharmaceutical Sciences, College of Pharmacy, Seoul National University, Seoul 08826, Republic of Korea*

Jin-Pyo An − *Korea Bioactive Natural Material Bank, Research Institute of Pharmaceutical Sciences, College of Pharmacy, Seoul National University, Seoul 08826, Republic of Korea*

Ba-Wool Lee − *Korea Bioactive Natural Material Bank, Research Institute of Pharmaceutical Sciences, College of Pharmacy, Seoul National University, Seoul 08826, Republic of Korea;* orcid.org/0000-0002-4944-5145

Jun-Li Yang − *Key Laboratory of Chemistry of Northwestern Plant Resources of CAS and Key Laboratory for Natural Medicine of Gansu Province, Lanzhou Institute of Chemical Physics, Chinese Academy of Sciences, Lanzhou 730000, People's Republic of China;* orcid.org/0000-0001-7199-0214

Complete contact information is available at: https://pubs.acs.org/10.1021/acs.jnatprod.9b00964

Author Contributions

H.-M. Cho and T.-K.-Q. Ha contributed equally to this work.

Notes

The authors declare no competing financial interest.

https://dx.doi.org/10.1021/acs.jnatprod.9b00964
J. Nat. Prod. 2020, 83, 2076−2086

■ ACKNOWLEDGMENTS

This work was supported financially in part by grants from the Bio & Technology Development (2016M3A9A5919548) and from the Basic Science Research Program (NRF-2017R1E1A1A01074674) through the National Research Foundation of Korea (NRF) funded by the Ministry of Education, Science, and Technology, Republic of Korea.

■ REFERENCES

(1) LaFerla, F. M.; Oddo, S. *Trends Mol. Med.* **2005**, *11*, 170−176.
(2) Seo, J. Y.; Pyo, E.; Park, J.; Kim, J. S.; Sung, S. H.; Oh, W. K. *J. Med. Food* **2017**, *20*, 1091−1099.
(3) Bojarski, L.; Herms, J.; Kuznicki, J. *Neurochem. Int.* **2008**, *52*, 621−633.
(4) Selvatici, R.; Marani, L.; Marino, S.; Siniscalchi, A. *Neurochem. Int.* **2013**, *63*, 112−120.
(5) Sastre, M.; Klockgether, T.; Heneka, M. T. *Int. J. Dev. Neurosci.* **2006**, *24*, 167−176.
(6) Uttara, B.; Singh, A. V.; Zamboni, P.; Mahajan, R. T. *Curr. Neuropharmacol.* **2009**, *7*, 65−74.
(7) Han, Y. S.; Zheng, W. H.; Bastianetto, S.; Chabot, J. G.; Quirion, R. *Br. J. Pharmacol.* **2004**, *141*, 997−1005.
(8) Kreutzberg, G. W. *Trends Neurosci.* **1996**, *19*, 312−318.
(9) McCarthy, R. C.; Lu, D. Y.; Alkhateeb, A.; Gardeck, A. M.; Lee, C. H.; Wessling-Resnick, M. *J. Neuroinflammation* **2016**, *13*, 21.
(10) Yu, Y.; Ye, R. D. *Cell. Mol. Neurobiol.* **2015**, *35*, 71−83.
(11) Nugroho, A.; Song, B. M.; Seong, S. H.; Chpo, J. S.; Choi, J.; Choi, J. Y.; Park, H. *Nat. Prod. Sci.* **2016**, *22*, 299−306.
(12) Yang, J. L.; Ha, T. K. Q; Dhodary, B.; Seo, J. Y.; Kim, H.; Park, J.; Oh, W. K. *Tetrahedron* **2016**, *72*, 3240−3249.
(13) Nakamura, S.; Moriura, T.; Park, S.; Fujimoto, K.; Matsumoto, T.; Ohta, T.; Matsuda, H.; Yoshikawa, M. *J. Nat. Prod.* **2012**, *75*, 1425−1430.
(14) Uddin, M. N.; Sharma, G.; Yang, J. L.; Choi, H. S.; Lim, S. I.; Kang, K. W.; Oh, W. K. *Phytochemistry* **2014**, *103*, 99−106.
(15) Yang, J. L.; Ha, T. K. Q.; Dhodary, B.; Pyo, E.; Nguyen, N. H.; Cho, H.; Kim, E.; Oh, W. K. *J. Med. Chem.* **2015**, *58*, 1268−1280.
(16) Cui, C.; Zong, J.; Sun, Y.; Zhang, L.; Ho, C.; Wan, Z.; Hou, R. *Food Funct.* **2018**, *9*, 3069−3091.
(17) Folch, J.; Petrov, D.; Ettcheto, M.; Abad, S.; Sanchez-Lopez, E.; Garcia, M. L.; Olloquequi, J.; Beas-Zarate, C.; Auladell, C.; Camins, A. *Neural Plast.* **2016**, *2016*, 1−15.
(18) Koirala, P.; Seong, S. H.; Jung, H. A.; Choi, J. S. *Asian Pac. J. Trop. Med.* **2017**, *10*, 1117−1122.
(19) Wagle, A.; Seong, S. H.; Zhao, B. T.; Woo, M. H.; Jung, H. A.; Choi, J. S. *Arch. Pharmacal Res.* **2018**, *41*, 409−418.
(20) Choi, R. J.; Roy, A.; Jung, H. J.; Ali, M. Y.; Min, B. S.; Park, C. H.; Yokozawa, T.; Fan, T. P.; Choi, J. S.; Jung, H. A. *J. Ethnopharmacol.* **2016**, *190*, 219−230.
(21) Palop, J. J.; Mucke, L. *Nat. Neurosci.* **2010**, *13*, 812−818.
(22) Revett, T. J.; Baker, G. B.; Jhamandas, J.; Kar, S. *J. Psychiatry Neurosci.* **2013**, *38*, 6−23.
(23) Kabogo, D.; Rauw, G.; Amritraj, A.; Baker, G.; Kar, S. *Neurobiol. Aging* **2010**, *31*, 1164−1172.
(24) Arias, C.; Arrieta, I.; Tapia, R. *J. Neurosci. Res.* **1995**, *41*, 561−566.
(25) Abe, K.; Misawa, M. *Brain Res.* **2003**, *979*, 179−187.
(26) Rodriguez-Kern, A.; Gegelashvili, M.; Schousboe, A.; Zhang, J.; Sung, L.; Gegelashvili, G. *Neurochem. Int.* **2003**, *43*, 363−370.
(27) Greenwood, S. M.; Connolly, C. N. *Neuropharmacology* **2007**, *53*, 891−898.
(28) Lipton, S. A. *NeuroRx* **2004**, *1*, 101−110.
(29) Beal, M. F. *Ann. Neurol.* **1995**, *38*, 357−366.
(30) Jin, M. C.; Yoo, J. M.; Sok, D. E.; Kim, M. R. *Neurochem. Res.* **2014**, *39*, 2440−2451.
(31) Fu, Y.; Koo, W. W. L. *Neurotoxic. Res.* **2006**, *10*, 23−29.
(32) Miranda, K. M.; Espey, M. G.; Wink, D. A. *Nitric Oxide* **2001**, *5*, 62−71.
(33) Aung, H. P.; Pyell, U. *J. Chromatogr. A* **2016**, *1449*, 156−165.
(34) Vasanits-Zsigrai, A.; Majercsik, O.; Tóth, G.; Csámpai, A.; Haveland-Lukács, C.; Pálfi, D.; Szadai, Z.; Rózsa, B.; Molnár-Perl, I. *J. Chromatogr. A* **2015**, *1394*, 81−88.

https://dx.doi.org/10.1021/acs.jnatprod.9b00964
J. Nat. Prod. 2020, 83, 2076−2086